Reversibility from DFT-Based Reactivity Indices: Intramolecular Side Reactions in the Polymerization of Poly(vinyl chloride)

Freija De Vleeschouwer,[†,||] Alejandro Toro-Labbé,[‡] Soledad Gutiérrez-Oliva,[‡] Veronique Van Speybroeck,[§,||] Michel Waroquier,[§,||] Paul Geerlings,[†,||] and Frank De Proft*[,†,||]

Eenheid Algemene Chemie (ALGC), Vrije Universiteit Brussel (VUB), Pleinlaan 2, 1050 Brussels, Belgium, Laboratorio de Química Teórica Computacional (QTC), Facultad de Química, Pontificia Universidad Católica de Chile, Santiago, Chile, and Center for Molecular Modeling (CMM), Ghent University (UGent), Proeftuinstraat 86, 9000 Gent, Belgium

Received: January 30, 2009; Revised Manuscript Received: May 3, 2009

A detailed investigation of the kinetic irreversibility−reversibility concept is presented on the basis of the analysis of four side reactions occurring in the polymerization of poly(vinyl chloride), the intramolecular 1,5- and 1,6-backbiting and 1,2- and 2,3-Cl shift side reactions. Density functional theory-based reactivity indices combined with an analysis of the reaction force are invoked to probe this concept. The reaction force analysis is used to partition the activation and reaction energy and characterize the behavior of reactivity indices along the three reaction regions that are defined within this approach. It has been observed that in the reactant and product regions mainly geometric rearrangements take place, whereas in the transition state region changes in the electronic bonding pattern occur; here most changes of the electronic properties are observed. The kinetic irreversibility−reversibility of the reactions is confirmed and linked to the differences in the Fukui function and dual descriptor of the radical centers associated with the initial and final species.

1. Introduction

Reversibility is an important concept in chemistry.[1] In a reversible reaction, the mechanism in one direction is exactly the reverse of the mechanism in the other direction.[1] Although all reactions are reversible to some extent, some reactions can be classified as irreversible. Thermodynamically, an irreversible reaction is a reaction that "goes to completion", which means that nearly all of the reactants are used to form products; in the case when both steps (i.e., the forward and reverse directions) are elementary, this corresponds to a kinetically irreversible reaction. Considerations of reversibility and irreversibility will be of utmost importance when considering (often undesired) side reactions in chemical processes. Indeed, when designing chemical transformations, it is hoped that side reactions will be either not present or at best reversible. It should also be noted that undesired products can still be formed even when a side reaction is reversible in the case when the side reaction is followed by a fast next step. In this contribution, we will study the "kinetic irreversibility" concept using DFT-based reactivity indices applied to different side reactions occurring in the synthesis of poly(vinyl chloride), an important polymer that is used in many applications. Indeed, despite its many good characteristics, such as its long lifetime and the fact that this material is easy to process, the low thermal stability of PVC caused by the occurrence of side reactions in the polymerization process remains a problem. These side reactions lead to structural defects within the polymer, which have a great impact on the characteristics of the product.[2] Better insight into the mechanism of these side reactions and their degree of reversibility would be helpful for improving the industrial production processes or, for PVC in particular, to reduce, for instance, the addition of environment-affecting thermal stabilizers during processing.[2] For more information about the structural and mechanistic aspects of thermal degradation of PVC, we refer to a recent review of Starnes.[3] Many other studies, both theoretical and experimental, have focused on the mechanisms of defect formation.[4−12] Very recently, a systematic study of all possible reaction routes that lead to structural defects in PVC, was performed by some of the authors.[13] On the basis of ab initio determined kinetic data and typical concentrations of monomer and polymer during suspension polymerization, the concentrations of all defects were theoretically derived. It supports the overall mechanism of defect formation, as previously established by the experiment.

The propagation step in the formation of PVC is the head-to-tail addition of the monomer unit (vinyl chloride) to the PVC radical (Scheme 1a). The side-reactions that lead to structural defects and that we will consider here are classified as intramolecular reactions. The main intramolecular reactions that may contribute to defects in the formation of PVC are the 1,5- and 1,6-backbiting reactions and the 1,2-Cl shift that may follow a head-to-head addition (Scheme 1b). These three irreversible reactions have been investigated in detail by some of the authors,[13] and the obtained ab initio data serve as input for further analysis in this work. Furthermore, we will also consider the 2,3-Cl shift that might follow a 1,2-Cl shift because of its reversible character. The backbiting reactions can take place only when the propagating radical consists of a minimum length of three monomer units. Both reactions occur through a curled-up transition state. The radical center at the end of the polymer abstracts a hydrogen atom from a neighboring carbon atom; as a result, the radical center moves up the chain. Further propagation leads to the following structural defects: butyl branches in the case of 1,5-backbiting and pentyl branches for

* Corresponding author. E-mail: fdeprof@vub.ac.be.
† Vrije Universiteit Brussel (VUB).
‡ Pontificia Universidad Católica de Chile.
§ Ghent University (UGent).
|| Member of the QCMM research group - Alliance Ghent-Brussels.

10.1021/jp900884z CCC: $40.75
Published on Web 06/12/2009

SCHEME 1: Reaction Mechanism of (a) the Head-to-Tail Propagation, (b) the 1,5-Backbiting, (c) the 1,6-Backbiting; (d) the 1,2-Cl Shift, and (e) the 2,3-Cl Shift

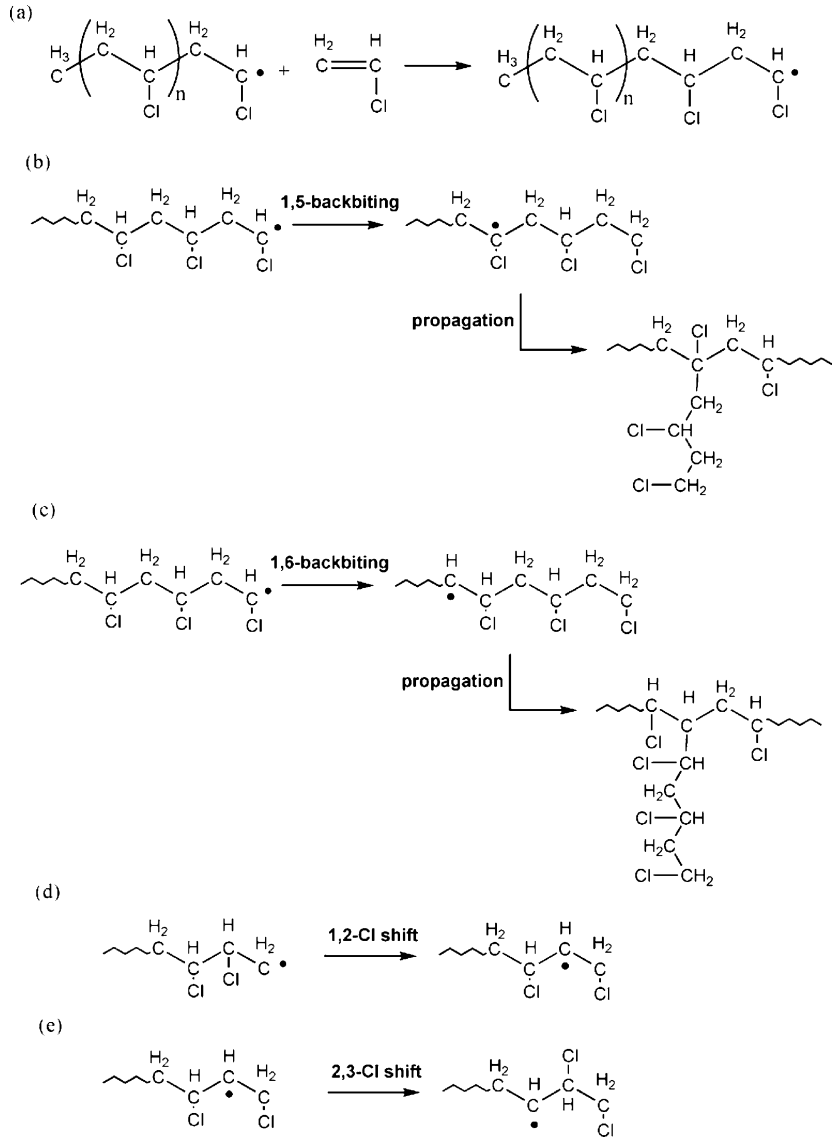

the 1,6-backbiting reaction (Scheme 1b,c). The 1,2-Cl shift (Scheme 1d) takes place after a head-to-head propagation that leaves two chlorine atoms bonded to carbon atoms in the α and β positions with respect to the radical center. The consecutive Cl shift happens very fast:[13] the radical center abstracts the chlorine atom on the α-carbon atom, leaving the latter to bear the unpaired electron. The 1,2-Cl shift introduces methyl branches, ethyl branches, and chloroallylic end groups depending on the next step in the polymerization scheme, that is, further propagation, second Cl shift (Scheme 1e), and Cl abstraction, respectively.[3,6,14−16]

The aim of this article is to investigate the reversibility−irreversibility property for these four intramolecular radical side reactions from two different and complementary perspectives. The first is the reaction force analysis,[17−21] which defines a framework for analyzing the second, that is, a set of different global and local electronic properties introduced within the context of "conceptual DFT".[22] In this contribution, the focus lies on two local reactivity descriptors: the Fukui function[23] and the dual descriptor for chemical reactivity.[24] This article is mainly intended to shed light on the mechanism and, more prominently, the (ir)reversibility of the backbiting reactions and the chlorine shifts through the simultaneous analysis of the above-mentioned properties using the reaction force analysis[17−21] that produces a fragmentation of the reaction coordinate into three reaction regions, each of them presenting its own characteristic pattern of evolution for the reactivity descriptors.

2. Theoretical Background

In this section, we will outline the different chemical concepts that will be used to probe the kinetic irreversibility of the aforementioned side reactions. The general framework for the analysis of the behavior of the different reactivity indices and the link of these observations with kinetic (ir)reversibility is the reaction force, obtained by differentiating the potential energy $E(\xi)$ with respect to ξ, the intrinsic reaction coordinate (IRC) expressed in mass-weighted Cartesian coordinates[19]

$$F(\xi) = -\frac{\partial E(\xi)}{\partial \xi} \tag{1}$$

The reaction force profile of any elementary step is characterized by two critical points that correspond to the inflection points

of the energy profile so that next to the known stationary points in a reaction path, that is, the reactant(s), the transition state, and the product(s), two extra key points are introduced: the minimum and maximum in the reaction force profile. These critical points define three reaction regions. The first and third regions are mostly characterized by geometric rearrangements, that is, preparation of the system for subsequent reaction and relaxation of the system; these are the so-called reactant(s) and product(s) regions, respectively. The actual transition to product(s), basically characterized by bond breaking and formation, occurs in the region between the two extrema in the reaction force profile. This is the transition-state region where electronic changes are predominant, which should be reflected by large changes of global and local electronic properties.

An important consequence of the fragmentation of the reaction coordinate into the three reaction regions is the rational partitioning of the activation and reaction energy. Introducing the positions ξ_R, ξ_0, and ξ_P of the reactant, transition state, and product and the positions ξ_{min} and ξ_{max} of the two extrema in the reaction force profile, the activation energy can be written as

$$\Delta E^{\neq} = W_1 + W_2 \tag{2}$$

with

$$W_1 = -\int_{\xi_R}^{\xi_{min}} F(\xi)\,d\xi \quad \text{and} \quad W_2 = -\int_{\xi_{min}}^{\xi_0} F(\xi)\,d\xi \tag{3}$$

Similarly, the reaction energy can be expressed as

$$\Delta E^0 = W_1 + W_2 + W_3 + W_4 \tag{4}$$

with

$$W_3 = -\int_{\xi_0}^{\xi_{max}} F(\xi)\,d\xi \quad \text{and} \quad W_4 = -\int_{\xi_{max}}^{\xi_P} F(\xi)\,d\xi \tag{5}$$

The reactivity indices that we will consider in this work and of which the behavior along the reaction coordinate will be linked to kinetic (ir)reversibility are the spin-polarized Fukui function and dual descriptor.[3] Profiles of the local reactivity indices along the reaction coordinate have been studied in previous publications,[25] although not within the framework of the kinetic reversibility−irreversibility issue.

Because intramolecular radical side reactions are investigated, in the most general case, a difference in α and β electron densities is present, whereas the total spin number, N_s (the difference between the total number of α and β electrons), remains constant along the reaction coordinate. We will thus compute and use the spin-polarized Fukui function, a DFT-based reactivity index probing the probability for a nucleophilic, electrophilic, or radical attack, for processes at constant spin number, f_{NN}.[26] This quantity is given by

$$f_{NN}(\mathbf{r}) = \left(\frac{\partial \rho(\mathbf{r})}{\partial N}\right)_{N_s,v(\mathbf{r})} \tag{6}$$

where the electron density, $\rho(\mathbf{r})$, is differentiated with respect to the number of electrons, N, at constant spin number, N_s, and external potential, $v(\mathbf{r})$ (and in absence of a magnetic field). This quantity was recently invoked in the investigation of the regioselectivity of radical cyclizations[27] and was also previously studied by nonspin resolved indices[28] and photonucleophilic aromatic substitution,[29] where it was computed in a frozen-core approximation[30] and condensed to the atoms[29] involved in the reaction. The Fukui function, f_{NN}, can be written in the $\{N_\alpha, N_\beta, v(\mathbf{r})\}$ representation using a set of four other Fukui functions[31]

$$f_{NN}(\mathbf{r}) = \frac{1}{2}[f_{\alpha\alpha}(\mathbf{r}) + f_{\alpha\beta}(\mathbf{r}) + f_{\beta\alpha}(\mathbf{r}) + f_{\beta\beta}(\mathbf{r})] \tag{7}$$

The Fukui functions in the $\{N_\alpha, N_\beta, v(\mathbf{r})\}$ representation are defined as follows

$$f_{\alpha\alpha}(\mathbf{r}) = \left(\frac{\partial \rho_\alpha(\mathbf{r})}{\partial N_\alpha}\right)_{N_\beta,v(\mathbf{r})}, \quad f_{\alpha\beta}(\mathbf{r}) = \left(\frac{\partial \rho_\alpha(\mathbf{r})}{\partial N_\beta}\right)_{N_\alpha,v(\mathbf{r})}, \quad f_{\beta\alpha}(\mathbf{r}) = \left(\frac{\partial \rho_\beta(\mathbf{r})}{\partial N_\alpha}\right)_{N_\beta,v(\mathbf{r})}, \quad f_{\beta\beta}(\mathbf{r}) = \left(\frac{\partial \rho_\beta(\mathbf{r})}{\partial N_\beta}\right)_{N_\alpha,v(\mathbf{r})} \tag{8}$$

where ρ_α and ρ_β are the densities of the α and β electrons, respectively. A detailed analysis of DFT-based reactivity indices in spin-resolved DFT, focusing in great detail on this representation, among others, was recently given by Pérez, Chamorro, and Ayers.[32]

The Fukui function for a radical attack is the average of the Fukui functions for a nucleophilic and an electrophilic attack

$$f^0_{NN}(\mathbf{r}) = \frac{f^+_{NN}(\mathbf{r}) + f^-_{NN}(\mathbf{r})}{2} \tag{9}$$

In 2004, Morell et al.[24] proposed a new descriptor for chemical reactivity, termed the dual descriptor. It is defined as the difference between the Fukui functions for a nucleophilic and an electrophilic attack

$$\Delta f(\mathbf{r}) = f^+(\mathbf{r}) - f^-(\mathbf{r}) \tag{10}$$

The new index is dual because electrophilic and nucleophilic regions within the molecule can be detected simultaneously. For a particular region in the molecule, $\Delta f(\mathbf{r}) > 0$ indicates that an electrophilic region has been determined and a nucleophilic attack is favored. On the other hand, if $\Delta f(\mathbf{r}) < 0$, then the region is nucleophilic and it may be prone to an electrophilic attack. This descriptor will be computed within the spin-polarized framework,[33] which is defined in terms of the corresponding constrained functions.

Note that all of the above Fukui functions can be condensed to atoms using electronic population analyses such as the natural population analysis (NPA).[34−36]

Finally, two remarks should be made. One should first notice that the reactivity indices studied in this article are optimal for studying orbital-controlled reactions, to which the present transformations studied belong. The analysis using the reaction

force concept could also be applied if one would treat a charge controlled reaction. In the case of the DFT-based reactivity indices, the concept of kinetic reversibility−irreversibility would then probably need to be assessed by considering another descriptor, such as the atomic charge, which is optimal for describing charge controlled reactions, as it was put forward in the contributions of ref 37.

Next, it should be noted that the reactions studied here are intramolecular processes. When intermolecular reactions are to be studied, one should use the local softness,[38] which is the product of the global softness with the Fukui function, instead of the Fukui function. Instead of the dual descriptor, in the case of intermolecular reactions, it will also be useful to use the recently proposed grand canonical dual descriptor,[39] or the so-called "multiphilic descriptor", defined as the difference between the nucleophilic and electrophilic condensed philicity functions.[40]

3. Computational Details

All calculations were performed within the Kohn−Sham framework using the Gaussian 03 program.[41] To get the profiles of the various properties evaluated in this article, we characterized the transition state for each intramolecular reaction, followed by an IRC calculation that connects the transition state with reactants and products; we made use of Becke's hybrid three-parameter functional B3LYP[42,43] with the standard 6-31+G* basis set.[44] Next, single-point energy calculations for all points along the IRC-profile were performed at the B3LYP/6-311+G** level of theory. For the computation of the condensed Fukui functions, atomic populations were obtained with the NPA method (also using the B3LYP-functional with basis set 6-311+G**), which is known to be reliable to calculate Fukui functions.[45] In view of the type of systems involved here (nonpolar halogenated alkyl radicals) and the type of reactions studied (intramolecular side reactions), it can expected that the influence of the solvent on the relationship between kinetic reversibility−irreversibility concept, on one hand, and the reactivity indices and the force profiles, on the other hand, will probably be small in this case. Detailed investigations of the effect of the solvent on the reaction force[46] and the reactivity indices[47] have been performed in the past.

4. Results and Discussion

The transition states associated with the four intramolecular side reactions displayed in Scheme 1 are presented in Figure 1. As can be seen from Figure 1a,b, the transition states of the 1,5- and 1,6-backbiting reaction are characterized by the formation of a six- and a seven-membered ring, respectively; the transition state for the 1,5-backbiting reaction is 13 kJ mol^{-1} more stable than that for the 1,6-backbiting reaction. The starting conformations for the backbiting reactions are the conformations of the radicals shown in Figure 2; they correspond to the closest local minima to the transition states. The 1,2- and 2,3-Cl shifts present a transition state in which the chlorine atom is practically midway between the carbon atoms (in question) (Figure 1c,d), whereas the propagating radical rearranges itself to form a saturated bond.

We will now systematically discuss the issue of kinetic (ir)reversibility for these four side reactions.

1,5-Backbiting. Figure 3a displays the potential energy profile of the 1,5-backbiting reaction. In the first part of the profile, the six-membered ring is being formed. After the transition state, a steeper slope is observed because a more stable secondary radical emerges. The energy barrier is 62.0 kJ mol^{-1} for the forward reaction and 75.3 kJ mol^{-1} for the reverse reaction, indicating that the 1,5-backbiting reaction is irreversible.

Figure 3b displays the reaction force profile, where the three reaction regions that constitute the framework for the subsequent analysis are defined. In the reactant region, C_5 bends toward the radical center at C_1, getting into position for the H shift. Around the minimum in force, the hydrogen detaches from the carbon atom and begins to float toward the radical center. Around the state of maximum force, the hydrogen binds to the radical center, and the system starts to relax to an equilibrium geometry.

The surface region bounded by the reaction force curve gives the energy cost/profit of the process. W_1 in zone 1 and W_4 in zone 3 are related to structural reordering, whereas W_2 and W_3 can be associated with electronic reordering. In the case of the 1,5-backbiting reaction, the contributions to the activation energy are $W_1 = 52.2$ kJ mol^{-1} and $W_2 = 9.8$ kJ mol^{-1}, thus indicating that 83% of the activation barrier should be associated with structural reordering that undergoes the backbone of the molecule to generate the six-membered ring structure that characterizes the transition state. The values of W_1 and W_4 (52.2 and 53.5 kJ mol^{-1}, respectively) indicate that the structural reordering needs about the same amount of work for the direct and the reverse process. Therefore, the kinetic irreversibility of the 1,5-backbiting reaction seems to be more related to electronic effects: the work W_3 (= 21.8 kJ mol^{-1}) for the reverse process is more than two times greater than W_2 (= 9.8 kJ mol^{-1}) for the direct reaction. Because the irreversibility can be explained through a difference in electronic reordering, this should be reflected in the profiles of the local reactivity descriptors.

In Figure 3c,d, the two local reactivity descriptors, f_{NN}^0 and Δf_{NN}, respectively, are shown. It can be observed that the most noticeable changes of these properties occur at the transition-state region; in the reactant and product regions, these quantities remain quite constant, thus confirming the fact that these regions are mainly characterized by structural changes. Concentrating first on the Fukui function, f_{NN}^0, the main changes occur to the radical center C_1 and to carbon C_5. In the electronic-driven transition state region, the Fukui function of the radical center C_1 indeed reduces very rapidly, as the hydrogen moves away from C_5 toward C_1. Carbon C_5 shows the opposite behavior. In the product region, the Fukui function reaches a constant level for both carbon atoms. The variation of f_{NN}^0 can be invoked to establish the kinetic irreversibility of the reaction: when the forward reaction has finished, the new radical center (C_5) becomes the most reactive site in the molecule, but it is still less reactive than the radical center C_1 in the reactant, thus inhibiting the reverse reaction. This result is completely in line with the results from the energetic data that show that the activation barrier for the reverse reaction ($\Delta E^{\neq}_{rev} = 75.3$ kJ mol^{-1}) is considerably larger than the barrier for the direct reaction ($\Delta E^{\neq} = 62.0$ kJ mol^{-1}).

The variation of the spin-polarized dual descriptor, as presented in Figure 3d, is equally interesting to examine. In the reactant region, the radical center C_1 is a strong electrophile; in the transition state region, the electrophilicity of this center decreases, whereas C_5 becomes more electrophilic. In the product region, the values of Δf_{NN} for both carbon atoms have approximately equalized. Again, this corresponds to the kinetical irreversibility of the reaction. The hydrogen is not likely to shift back to C_1 because the electrophilicity of the two carbon atoms is about the same. Also, the reactivity of the chlorine atoms remains fairly unchanged all along the reaction path.

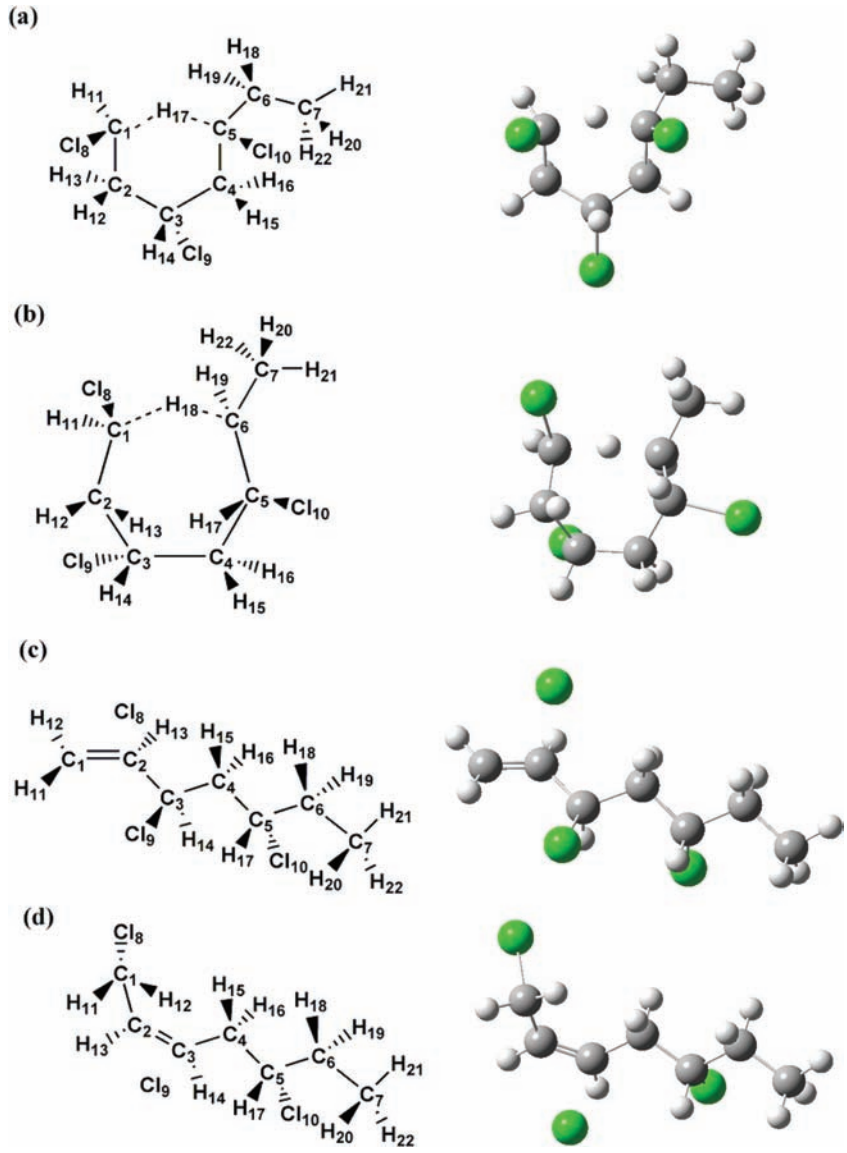

Figure 1. Transition state of (a) the 1,5-backbiting, (b) the 1,6-backbiting, (c) the 1,2-Cl shift, and (d) the 2,3-Cl shift.

1,6-Backbiting. Not surprisingly, the potential energy profile in Figure 4a for the 1,6-backbiting reaction is similar to the profile obtained for the 1,5-backbiting reaction because both transitions to products involve a cyclization process. Figure 4b displays the reaction force profile and defines again the reaction regions that are indicated by the vertical lines on the Figures; the partitioning of the activation energy in terms of W_1 and W_2 emerges naturally. The 1,6-backbiting reaction is found to be irreversible, when considering the high energy barrier of the reverse process ($\Delta E^{\neq}_{rev} = 76.7$ kJ mol^{-1}) in comparison with the lower barrier of the direct reaction ($\Delta E^{\neq} = 66.3$ kJ mol^{-1}). The structural rearrangements of the system for the forward reaction of the 1,6-backbiting reaction take about the same amount of work ($W_1 = 52.5$ kJ mol^{-1}) as that for the 1,5-backbiting reaction ($W_1 = 52.2$ kJ mol^{-1}). For the reverse process, less work is needed for the geometric relaxation of the system with a value of 46.9 kJ mol^{-1} for W_4. However, as was the case for the 1,5-backbiting reaction, the main differences between the forward and reverse processes are due to electronic effects, as confirmed by the values for W_2 (= 13.8 kJ mol^{-1}) and W_3 (= 29.8 kJ mol^{-1}): the work for the electronic reordering of the reverse reaction is more than twice as large as that for the forward reaction. The components of the activation energy, $W_1 = 52.5$ kJ mol^{-1} and $W_2 = 13.8$ kJ mol^{-1}, indicate that, as for the 1,5-backbiting reaction, the energy associated with structural rearrangements (W_1) constitutes most of the activation energy (79%). However, a rise in the electronic effects is observed with respect to the 1,5-backbiting reaction because it makes up 21% of the activation energy of the 1,6-backbiting reaction.

The variation of the spin-polarized Fukui function in Figure 4c is again localized at the transition-state region, with the most significant changes for carbon atoms C_1 and C_6. C_1 experiences an enormous decrease in reactivity and, as expected, the future radical center C_6 displays the inverse behavior. The findings agree with the 1,5-backbiting reaction, pointing out the similarity between both reactions. However, when the explicit values of f_{NN}^0 for the original radical center are compared for both backbiting reactions, one remarks that C_1 is less reactive in the case of the 1,6-backbiting reaction, which is consistent with a higher energy barrier for this reaction (66.3 kJ mol^{-1} compared with 62.0 kJ mol^{-1} for 1,5-backbiting). In addition, the future radical center displays less reactive character than the original radical center when comparing the values of f_{NN}^0, indicating that

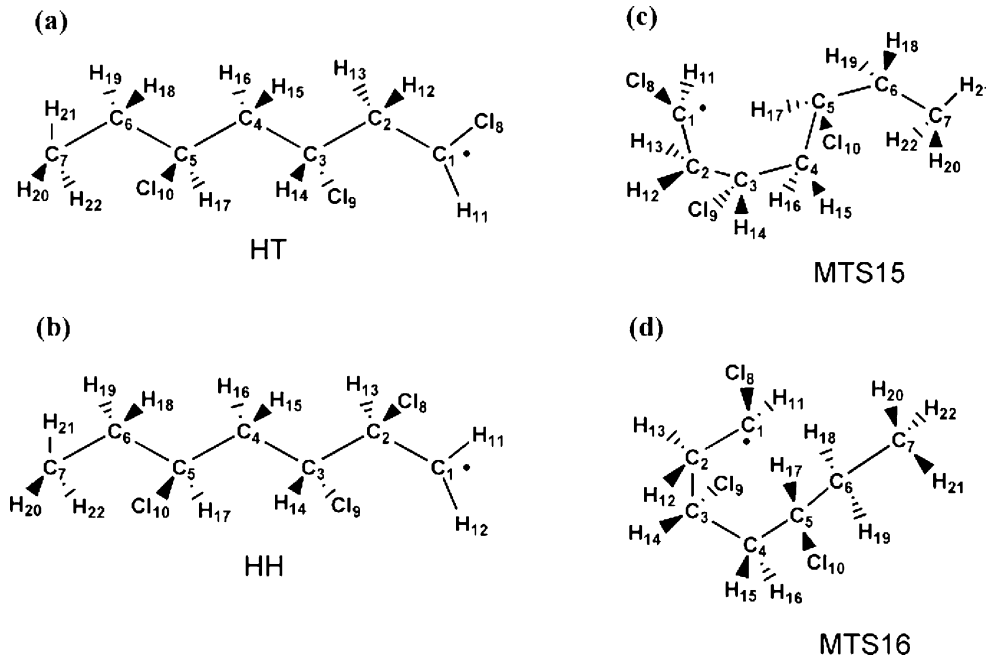

Figure 2. (a) The head-to-tail syndiotactic straight chain 3 M.U. (monomer units) (HT), (b) the head-to-head chain 3 M.U. (HH), (c) the minimum close to the transition state of the 1,5-backbiting reaction 3 M.U. (MTS15), and (d) the minimum close to the transition state of the 1,6-backbiting reaction 3 M.U. (MTS16).

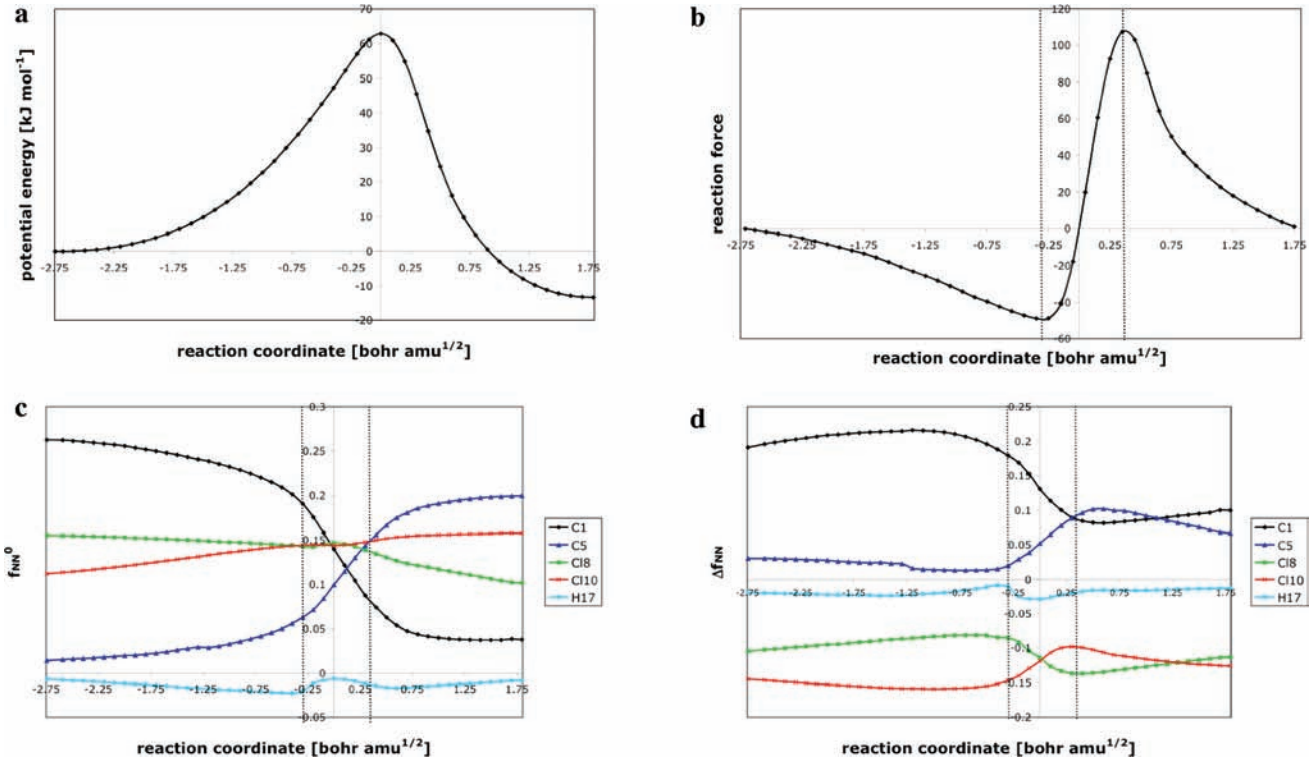

Figure 3. Potential energy, reaction force, and reactivity descriptors along the reaction path of the 1,5-backbiting reaction: (a) potential energy, (b) reaction force, (c) spin-polarized Fukui function, and (d) spin-polarized dual descriptor.

the backbiting process is irreversible. We remark that the difference in the spin-polarized Fukui function between the original and future radical centers is larger for the 1,5-backbiting reaction than for the 1,6-backbiting, which explains the larger difference in the reaction barrier for the forward and reverse reactions of the former.

The spin-polarized dual descriptor in Figure 4d shows that the original radical center is the most electrophilic atom in the reactant conformation. Again, an equalization of the electrophilicity of both carbon atoms (C_1 and C_6) occurs in the product region, so there is no tendency for the hydrogen to shift back. Moreover, a large reduction in the value of Δf_{NN} is detected when comparing the radical center in the initial (C_1) and final (C_6) configurations, backing up the kinetic irreversibility of the 1,6-backbiting reaction.

1,2-Chlorine Shift. As will be seen, the 1,2-Cl shift is different from the backbiting reactions, resulting in a different behavior of the properties under study; compared with the

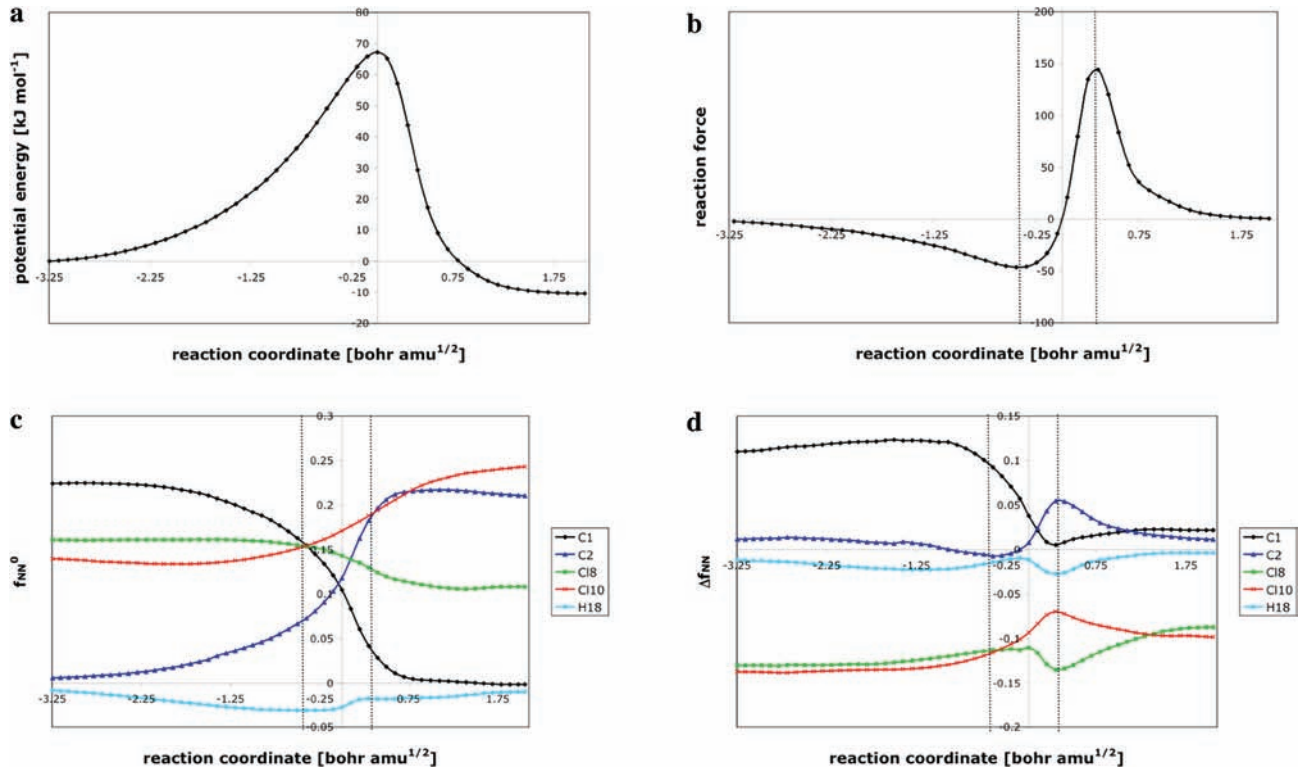

Figure 4. Potential energy, reaction force, and reactivity descriptors along the reaction path of the 1,6-backbiting reaction: (a) potential energy, (b) reaction force, (c) spin-polarized Fukui function, and (d) spin-polarized dual descriptor.

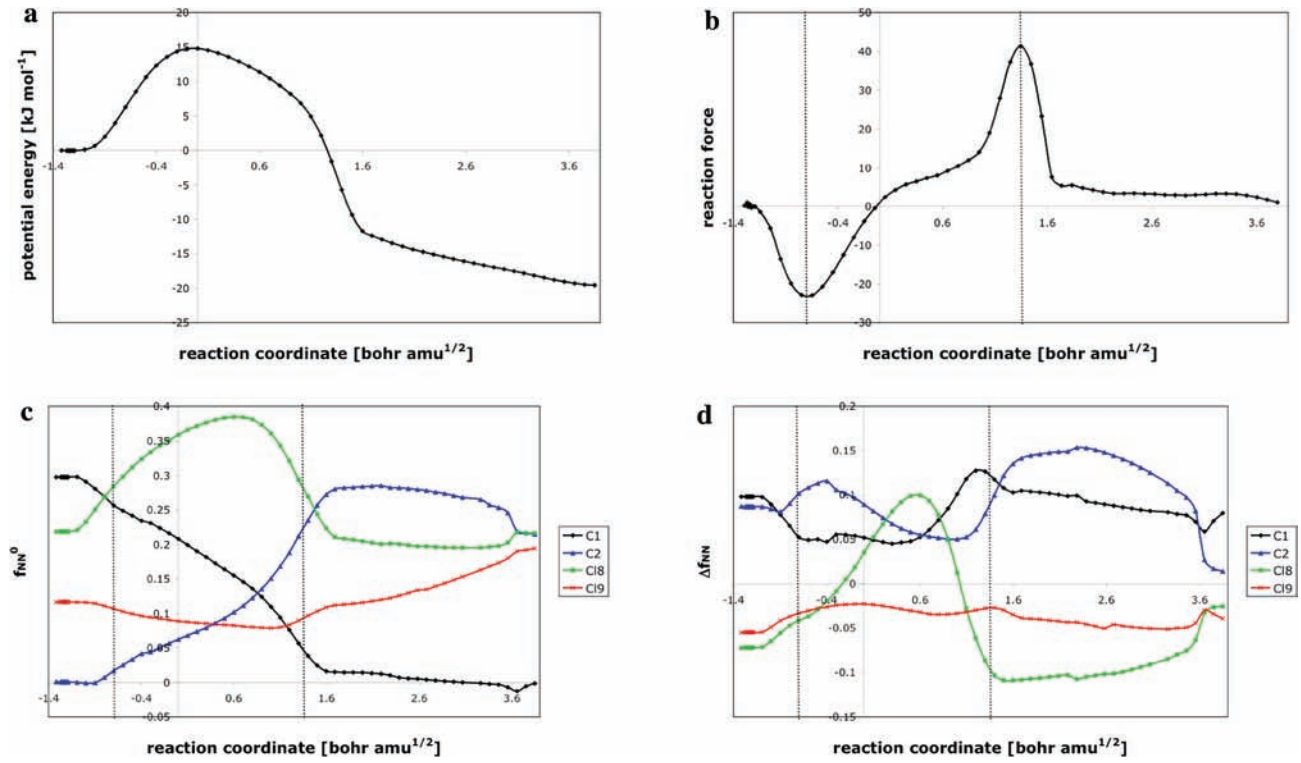

Figure 5. Potential energy, reaction force, and reactivity descriptors along the reaction path of the 1,2-Cl shift: (a) potential energy, (b) reaction force, (c) spin-polarized Fukui function, and (d) spin-polarized dual descriptor.

backbiting reactions, the main feature is the quite broad maximum observed at the transition state, as can be seen from Figure 5a, indicating the importance of electronic effects for this type of reaction. Figure 5b shows the reaction force for the entire reaction path and the corresponding reaction regions.

It can be stated that this reaction is largely irreversible; $\Delta E^{\neq}_{rev} = 34.4$ kJ mol^{-1} is more than twice the activation energy $\Delta E^{\neq} = 14.8$ kJ mol^{-1} for the direct reaction. Contrary to the backbiting reactions, both direct and reverse barriers present quite balanced energetic contributions of structural and electronic

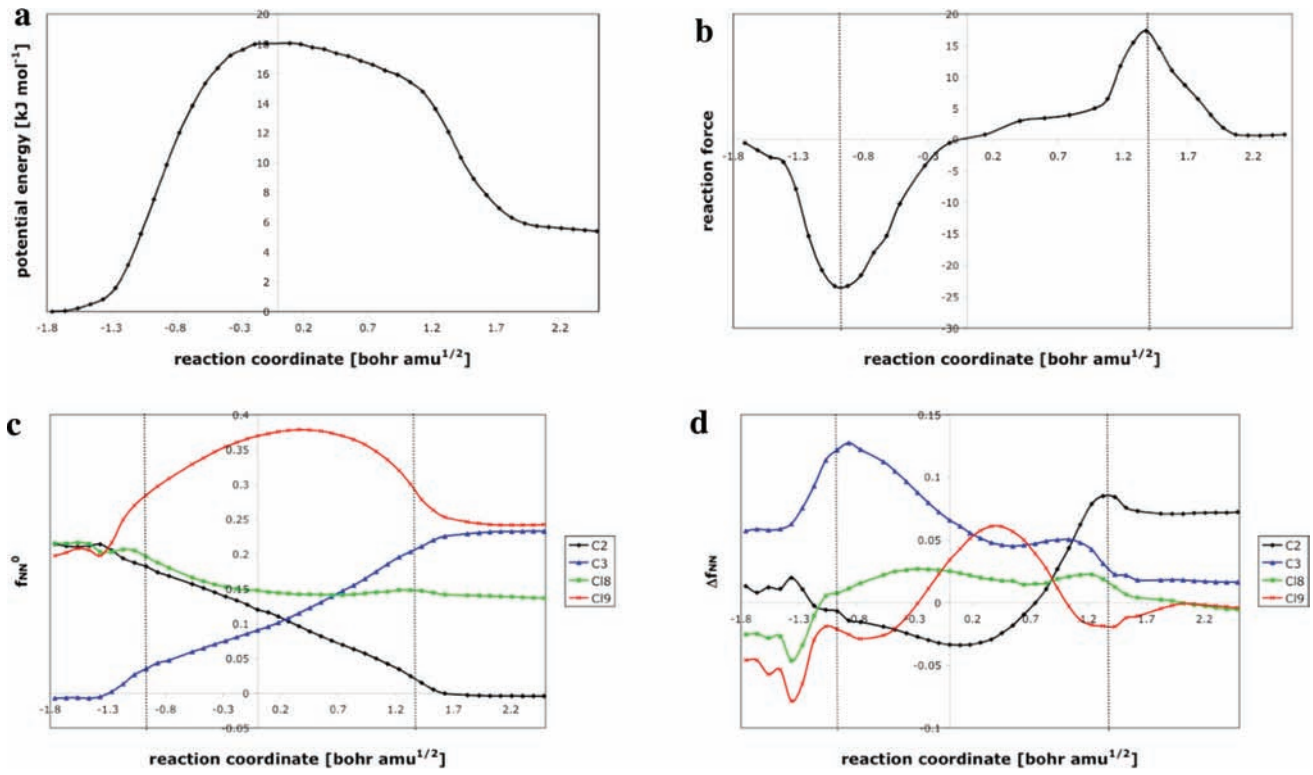

Figure 6. Potential energy, reaction force, and reactivity descriptors along the reaction path of the 2,3-Cl shift: (a) potential energy, (b) reaction force, (c) spin-polarized Fukui function, and (d) spin-polarized dual descriptor.

nature. For the direct reaction, the composition of the activation energy is 42% of structural nature and 58% of electronic nature; for the reverse barrier, these are 46 and 54%, respectively. The relative weight of the electronic effects is more important than that in the previous backbiting reactions, stressing the different nature of the 1,2-chlorine shift.

Figure 5c displays the variation of the spin-polarized Fukui function. In the transition-state region, a strong decrease in the reactivity of the radical center C_1 takes place. Once chlorine atom Cl_8 is attached, f_{NN}^0 remains constant, despite the subsequent internal rotation over the C_2-C_3 axis. The reactivity of C_2, that is, the future radical center, increases in the electronic-driven zone. However, the subsequent internal rotation causes the carbon atom to become less reactive. In the product configuration, the two chlorine atoms, Cl_8 and Cl_9, as well as carbon C_2 appear to be about equally reactive but still less compared with the value of f_{NN}^0 for C_1 in the reactant. This confirms the fact that the 1,2-Cl shift is an irreversible reaction. On the basis of the HSAB principle,[48,49] the similar reactivity of Cl_9 and C_2 indicates the possibility of a second Cl shift, as is confirmed in the literature[13] and which will be discussed later on.

The profile of the spin-polarized dual descriptor in Figure 5d is far more complicated. In the reactant region, the bond distance of Cl_8 and C_2 increases, resulting in the diminishing nucleophilicity of the chlorine atom, whereas the carbon atom becomes more electrophilic. This behavior continues until the bond between Cl_8 and C_2 is completely broken and the chlorine atom starts acting as a radical. From that moment on, Cl_8 looses its nucleophilic character and becomes an electrophile. In the transition-state region, symmetry is more or less present. Now, when the chlorine radical starts to bind to C_1, it is restored as a nucleophilic site. Meanwhile, the new radical center C_2 has become a strong electrophile. The product region is related to the internal rotation over the C_2-C_3 axis that causes a major decrease in the electrophilicity of carbon atom C_2, which becomes even less than the electrophilicity of carbon atom C_1, as well as an enormous reduction in the nucleophilicity of Cl_8. On the grounds of the intuitively defined relationship between nucleophilicity and electrophilicity, it is therefore not likely that the reverse Cl shift will take place, which is again consistent with literature[13] and which thus confirms the irreversibility of the 1,2-Cl shift.

2,3-Chlorine Shift. The 2,3-Cl shift is very similar to the 1,2-Cl shift. Again, the potential energy profile in Figure 6a is characterized by a very broad maximum around the transition state. In Figure 6b the reaction force for the entire reaction path and the corresponding reaction regions are shown. A comparison of the activation energies for the forward (= 17.8 kJ mol^{-1}) and reverse (= 12.4 kJ mol^{-1}) reactions shows that the 2,3-Cl shift is kinetically reversible. This is to be expected because the original and the newly formed radical centers are both secondary radicals. The small energy difference is probably due to the fact that in the product the two chlorine atoms Cl_8 and Cl_9 are bonded to neighboring carbon atoms, enhancing the repulsive effect. As was the case with the 1,2-Cl shift, structural and electronic effects have more or less an equal influence on the composition of the energy barrier. For the forward reaction, 43% of the activation energy can be contributed to structural changes, and thus 57% can be contributed to electronic effects; for the reverse reaction, the contributions are 45% and 55% of structural and electronic nature, respectively.

In Figure 6c, the spin-polarized Fukui function is plotted along the reaction path. In the reactant and product regions, the descriptor remains fairly constant for all atoms under consideration. In the transition-state region, however, f_{NN}^0 rapidly

decreases for carbon atom C_2, the original radical center, and increases by about the same amount for carbon atom C_3, the future radical center. Indeed, the original radical center in the reactant and the future radical center in the product display more or less the same reactivity, indicating that the 2,3-Cl shift is kinetically reversible. Figure 6d shows the profile of the spin-polarized dual descriptor. In the begin and end configuration, about the same difference in value of Δf_{NN} for the original and future radical centers with respect to chlorine atom Cl_9 is encountered. Therefore, there is no indication that the reverse reaction is prohibited.

5. Concluding Remarks

(Kinetic) reversibility−irreversibility is an important concept in chemistry, for example, in the area of polymer chemistry where controlling and, more specifically, the hindering of side reactions plays an important role. To probe this concept from the viewpoint of reactivity indices, the mechanism of four intramolecular side reactions in the polymerization scheme of poly(vinyl chloride), namely, the 1,5- and 1,6-backbiting reactions and the 1,2- and 2,3-Cl shift reactions, were studied, with the main focus on the reversibility−irreversibility issue. The partitioning of the activation and reaction energy on the basis of the reaction force concept gives a very good indication of whether the irreversibility of the side reaction can be attributed to structural or electronic effects or a combination of both. Moreover, it is shown that the Fukui function as well as the dual descriptor can be used to rationalize the kinetic irreversibility of the considered reactions. For all irreversible side reactions (the 1,2-Cl shift and the 1,5- and the 1,6-backbiting reactions), the Fukui function value, that is, the reactivity, of the original radical center was higher than that of the product radical center, and thus the reverse reaction is less likely. In addition, for the backbiting reactions, an equalization of the dual descriptor for the original and product radical centers was observed, whereas for the 1,2-Cl shift, the value of the dual descriptor of the original radical center in the product conformation is higher than the value for the product radical center. In all of these cases, there is no driving force for the reverse pathway. The only reversible side reaction, that is, the 2,3-Cl shift, shows different behavior: about the same difference in value of dual descriptor for the original radical center in the reactant conformation and the product radical center in the product conformation with respect to the chlorine atom is encountered.

Acknowledgment. F.D.V. and F.D.P. acknowledge financial support from a Research Program of the Research Foundation - Flanders (FWO) (G.0464.06). V.V.S. and M.W. thank the Fund for Scientific Research Flanders (FWO) and the Research Board of the Ghent University. A.T.-L. thanks FONDECYT for the financial support through project 1060590 and FONDAP for the financial support through project 11980002 (CIMAT). S. G.-O. thanks FONDECYT for the financial support through project 11070197.

References and Notes

(1) *IUPAC Compendium of Chemical Terminology*, 2nd ed.; McNaught, A. D., Wilkinson, A., Ed.; Blackwell Scientific Publications: Oxford, U.K., 1997.
(2) Endo, K. *Prog. Polym. Sci.* **2002**, *27*, 2021.
(3) Starnes, W. H. *Prog. Polym. Sci.* **2002**, *27*, 2133.
(4) Xie, T. Y.; Hamielec, A. E.; Rogestedt, M.; Hjertberg, T. *Polymer* **1994**, *35*, 1526–1534.
(5) Hjertberg, T.; Sorvik, E. M. *Polymer* **1983**, *24*, 673.
(6) Purmova, J.; Pauwels, K. F. D.; van Zoelen, W.; Vorenkamp, E. J.; Schouten, A. J.; Coote, M. L. *Macromolecules* **2005**, *38*, 6352.
(7) d'Antuono, P.; Botek, E.; Champagne, B.; Wieme, J.; Reyniers, M. F.; Marin, G. B.; Adriaensens, P. J.; Gelan, J. M. *Chem. Phys. Lett.* **2005**, *411*, 207.
(8) De Roo, T.; Wieme, J.; Heynderickx, G. J.; Marin, G. B. *Polymer* **2005**, *46*, 8340.
(9) Izgorodina, E. I.; Coote, M. L. *Chem. Phys.* **2006**, *324*, 96.
(10) d'Antuono, P.; Botek, E.; Champagne, B.; Wieme, J.; Reyniers, M. F.; Marin, G. B.; Adriaensens, P. J.; Gelan, J. M. *Chem. Phys. Lett.* **2007**, *436*, 388.
(11) Wieme, J.; Marin, G. B.; Reyniers, M. F. *Chem. Eng. Sci.* **2007**, *62*, 5300.
(12) d'Antuono, P.; Botek, E.; Champagne, B.; Wieme, J.; Reyniers, M. F.; Marin, G. B.; Adriaensens, P. J.; Gelan, J. M. *J. Phys. Chem. B* **2008**, *112*, 14804.
(13) Van Cauter, K.; Van den Bossche, B. J.; Van Speybroeck, V.; Waroquier, M. *Macromolecules* **2007**, *40*, 1321.
(14) Starnes, W. H.; Schilling, F. C.; Abbas, K. B.; Cais, R. E.; Bovey, F. A. *Abstr. Pap. Am. Chem. Society.* **1979**, 144.
(15) Starnes, W. H. *J. Polym. Sci., Part A: Polym. Chem.* **2005**, *43*, 2451.
(16) Rigo, A.; Talamini, G.; Palma, G. *Makromol. Chem.* **1972**, *153*, 219.
(17) Toro-Labbé, A. *J. Phys. Chem. A* **1999**, *103*, 4398.
(18) Jaque, P.; Toro-Labbé, A. *J. Phys. Chem. A* **2000**, *104*, 995.
(19) Politzer, P.; Toro-Labbé, A.; Gutierrez-Oliva, S.; Herrera, B.; Jaque, P.; Concha, M. C.; Murray, J. S. *J. Chem. Sci.* **2005**, *117*, 467.
(20) Toro-Labbé, A.; Gutierrez-Oliva, S.; Concha, M. C.; Murray, J. S.; Politzer, P. *J. Chem. Phys.* **2004**, *121*, 4570.
(21) Herrera, B.; Toro-Labbé, A. *J. Chem. Phys.* **2004**, *121*, 7096.
(22) (a) Parr, R. G.; Yang, W. *Density Functional Theory of Atoms and Molecules*; Oxford University Press: New York, 1989. (b) Parr, R. G.; Yang, W. *Annu. Rev. Phys. Chem.* **1995**, *46*, 701. (c) Kohn, W.; Becke, A. D.; Parr, R. G. *J. Phys. Chem.* **1996**, *100*, 12974. (d) Geerlings, P.; De Proft, F.; Langenaeker, W. *Adv. Quantum Chem.* **1999**, *33*, 303. (e) Chermette, H. *J. Comput. Chem.* **1999**, *20*, 129. (f) Geerlings, P.; De Proft, F.; Langenaeker, W. *Chem. Rev.* **2003**, *103*, 1793. (g) Ayers, P. W.; Anderson, J. S. M.; Bartolotti, L. J. *Int. J. Quantum Chem.* **2005**, *101*, 520.
(23) Parr, R. G.; Yang, W. T. *J. Am. Chem. Soc.* **1984**, *106*, 4049.
(24) Morell, C.; Grand, A.; Toro-Labbe, A. *J. Phys. Chem. A* **2005**, *109*, 205.
(25) (a) Chattaraj, P. K.; Roy, D. R. *J. Phys. Chem. A* **2005**, *109*, 3771. (b) Chattaraj, P. K.; Roy, D. R. *J. Phys. Chem. A* **2006**, *110*, 11401.
(26) Galvan, M.; Vela, A.; Gazquez, J. L. *J. Phys. Chem.* **1988**, *92*, 6470.
(27) Pinter, B.; De Proft, F.; Van Speybroeck, V.; Hemelsoet, K.; Waroquier, M.; Chamorro, E.; Veszpremi, T.; Geerlings, P. *J. Org. Chem.* **2007**, *72*, 348.
(28) Hemelsoet, K.; Van Speybroeck, V.; Marin, G. B.; De Proft, F.; Geerlings, P.; Waroquier, M. *J. Phys. Chem. A* **2004**, *108*, 7281.
(29) Pinter, B.; De Proft, F.; Veszpremi, T.; Geerlings, P. *J. Org. Chem.* **2008**, *73*, 1243. (2008).
(30) Chamorro, E.; Pérez, O. *J. Chem. Phys.* **2005**, *123*, 114107.
(31) Garza, J.; Vargas, R.; Cedillo, A.; Galvan, M.; Chattaraj, P. K. *Theor. Chem. Acc.* **2006**, *115*, 257.
(32) Pérez, P.; Chamorro, E.; Ayers, P. W. *J. Chem. Phys.* **2008**, *128*, 204108.
(33) Chamorro, E.; Pérez, P.; Duque, M.; De Proft, F.; Geerlings, P. *J. Chem. Phys.* **2008**, *129*, 064117.
(34) Reed, A. E.; Weinstock, R. B.; Weinhold, F. *J. Chem. Phys.* **1985**, *83*, 735.
(35) Reed, A. E.; Weinhold, F. *J. Chem. Phys.* **1985**, *83*, 1736.
(36) Reed, A. E.; Curtiss, L. A.; Weinhold, F. *Chem. Rev.* **1988**, *88*, 899.
(37) (a) Melin, J.; Aparicio, F.; Subramanian, V.; Galván, M.; Chattaraj, P. K. *J. Phys. Chem. A* **2004**, *108*, 2487. (b) Chattaraj, P. K. *J. Phys. Chem. A* **2001**, *105*, 511. (c) Klopman, G. *J. Am. Chem. Soc.* **1968**, *90*, 223.
(38) Lee, C.; Yang, W.; Parr, R. G. *THEOCHEM* **1988**, *163*, 305.
(39) Ayers, P. W.; Morell, C.; De Proft, F.; Geerlings, P. *Chem.−Eur. J.* **2007**, *13*, 8240.
(40) Padmanabhan, J.; Parthasarathi, R.; Elango, M.; Subramanian, V.; Krishnamoorthy, B. S.; Gutierrez-Oliva, S.; Toro-Labbé, A.; Roy, D. R.; Chattaraj, P. K. *J. Phys. Chem. A* **2007**, *111*, 9130.
(41) Frisch, M. J.; Trucks, G. W.; Schlegel, H. B.; Scuseria, G. E.; Robb, M. A.; Cheeseman, J. R.; Montgomery, J. A., Jr.; Vreven, T.; Kudin, K. N.; Burant, J. C.; Millam, J. M.; Iyengar, S. S.; Tomasi, J.; Barone, V.; Mennucci, B.; Cossi, M.; Scalmani, G.; Rega, N.; Petersson, G. A.; Nakatsuji, H.; Hada, M.; Ehara, M.; Toyota, K.; Fukuda, R.; Hasegawa, J.; Ishida, M.; Nakajima, T.; Honda, Y.; Kitao, O.; Nakai, H.; Klene, M.; Li, X.; Knox, J. E.; Hratchian, H. P.; Cross, J. B.; Bakken, V.; Adamo, C.; Jaramillo, J.; Gomperts, R.; Stratmann, R. E.; Yazyev, O.; Austin, A. J.;

Cammi, R.; Pomelli, C.; Ochterski, J. W.; Ayala, P. Y.; Morokuma, K.; Voth, G. A.; Salvador, P.; Dannenberg, J. J.; Zakrzewski, V. G.; Dapprich, S.; Daniels, A. D.; Strain, M. C.; Farkas, O.; Malick, D. K.; Rabuck, A. D.; Raghavachari, K.; Foresman, J. B.; Ortiz, J. V.; Cui, Q.; Baboul, A. G.; Clifford, S.; Cioslowski, J.; Stefanov, B. B.; Liu, G.; Liashenko, A.; Piskorz, P.; Komaromi, I.; Martin, R. L.; Fox, D. J.; Keith, T.; Al-Laham, M. A.; Peng, C. Y.; Nanayakkara, A.; Challacombe, M.; Gill, P. M. W.; Johnson, B.; Chen, W.; Wong, M. W.; Gonzalez, C.; Pople, J. A. *Gaussian 03*, revision B.03; Gaussian, Inc.: Wallingford, CT, 2004.

(42) Becke, A. D. *J. Chem. Phys.* **1993**, *98*, 5648.

(43) Lee, C. T.; Yang, W. T.; Parr, R. G. *Phys. Rev. B* **1988**, *37*, 785.

(44) For a detailed account on these types of basis sets, see, for example: Hehre, W. J.; Radom, L.; Schleyer, P. v. R.; Pople, J. A. *Ab Initio Molecular Orbital Theory*; Wiley: New York, 1986.

(45) De Proft, F.; Martin, J. M. L.; Geerlings, P. *Chem. Phys. Lett.* **1996**, *256*, 400.

(46) Burda, J. V.; Toro-Labbé, A.; Gutirrez-Oliva, S.; Murray, J. S.; Politzer, P. *J. Phys. Chem. A* **2007**, *111*, 2455.

(47) For a recent analysis and an account of previous studies, see: Jaramillo, P.; Pérez, P.; Fuentealba, P.; Canuto, S.; Coutinho, K. *J. Phys. Chem. B* **2009**, *113*, 4314.

(48) (a) Pearson, R. G. *Hard and Soft Acids and Bases*; Dowden, Hutchinson, & Ross: Stroudenbury, PA, 1973. (b) Pearson, R. G. *Chemical Hardness*; Wiley-VCH: Weinheim, Germany, 1997.

(49) For a local version of this principle, see, for example: Gazquez, J. L.; Mendez, F. *J. Phys. Chem.* **1994**, *98*, 4591.

JP900884Z